POLISH MARITIME RESEARCH 4 (124) 2024 Vol. 31; pp. 31-42
10.2478/pomr-2024-0048

Development and Validation of a Wave-Propelled Semi-submersible Unmanned Vehicle

Yingyuan Tian [1,2]
Weijia Li [1]*
Zhigang Wang [3]
[1] School of Naval Architecture and Ocean Engineering, Huazhong University of Science and Technology. Wuhan, Hubei, China
[2] Qingdao Innovation and Development Center of Harbin Engineering University. Qingdao, Shandong, China
[3] Yichang Testing Technique Research Institute. Yichang, Hubei, China

* Corresponding author: *liweijia@hust.edu.cn (Weijia Li)*

ABSTRACT

Ocean observation and exploration technologies are crucial for marine environmental protection and resource development, but traditional tools have limitations in terms of operating time, coverage, and cost. Wave gliders, which offer advantages such as long duration, wide range, and low cost, are a promising solution, but their low speed and weak manoeuvrability hinder their application, due to poor collision avoidance and survivability. This study proposes a novel wave-propelled semi-submersible unmanned vehicle (WPSUV) to overcome these disadvantages. The WPSUV features a submerged main structure for navigation and autonomous collision avoidance through rapid buoyancy adjustment. Modelling, computational hydrodynamic and motion simulations, and functional and performance testing at sea demonstrate the feasibility and superior performance of the WPSUV compared to conventional wave gliders. The proposed WPSUV significantly enhances collision avoidance through diving, reduced visual target and wind resistance with minimal structures above the waterline, and improved stability due to its lower centre of gravity. This slightly positively buoyant vehicle with a high lift-to-drag ratio can effectively harness wave kinetic energy and achieve favourable wave-following characteristics. In addition, the submerged main structure provides protection against surface hazards and allows for stealthy operation. This novel wave-propelled and near-surface unmanned underwater vehicle has the potential to revolutionise marine observation and exploration, and to enable safe, reliable, and long-term monitoring of the marine environment.

Keywords: Wave propelled semi-submersible unmanned vehicle (WPSUV); Marine observation; Collision avoidance; Unmanned underwater vehicle (UUV); Wave glider

INTRODUCTION

Unmanned and autonomous marine robots represent a burgeoning field within marine robotics, as they have a range of applications across diverse domains, including marine scientific research, engineering construction, resource development, and national defence [1]-[3]. However, conventional marine unmanned vehicles often suffer from endurance limitations due to energy constraints, impeding their capability for sustained, large-scale, and cost-efficient operations at sea. Natural energy propulsion has emerged as a promising solution to augment the endurance of marine unmanned vehicles [4].

Wave-energy-driven unmanned vehicles are distinguished by prolonged endurance, cost-effectiveness, and minimal navigation noise [5], and wave gliders in particular have been noted for these advantages. In the realm of marine environmental protection, they can be used for purposes such as water quality monitoring, pollution detection, and marine species tracking.

Their autonomous operation over extended durations enables data collection in remote and inaccessible regions. With a focus on the area of marine meteorological and water quality observations, the authors of [6] used wave gliders to make high-resolution wind speed measurements in the field, and compared them with several wind speed data products. In [7], methods of measuring waves and winds from a wave glider were studied, while in [8], wave gliders were used to provide comprehensive, continuous and long-term monitoring of marine water quality. The authors of [9] achieved timely, continuous, and high-accuracy estimation and monitoring of centimetre-scale vertical seafloor motions with a wave glider. As one aspect of a marine biological survey, the researchers in [10] deployed an innovative array of imaging and photophysiological sensors for the Honey Badger wave glider that were specifically designed to monitor phytoplankton dynamics. This deployment aimed to investigate the circulation patterns of diatom blooms in the eastern North Pacific during the summer season. In [11], a wave glider was used to autonomously track an oceanic thermal front known to have biological importance and to undergo dynamic evolution. A wave glider was also equipped with passive acoustic listening equipment to detect fish sounds and to study the dynamics of fish populations [12]. In the domain of communications, positioning and target detection, the study in [13] presented an architecture for an Internet of Underwater Things (IoUT), involving multiple wave gliders as nodes for an acoustic observation and target localisation method.

Despite their inherent advantages, current wave glider technologies face a range of challenges, including limitations on their speed, manoeuvrability, and concealment. These constraints compromise their ability to effectively evade active damage, thereby jeopardising their overall survivability.

Modelling and simulation of wave dynamics for near-surface navigation of underwater vehicles is crucial in terms of understanding their motion stability, manoeuvrability, and efficiency. The authors of [14] computed wave forces and moments for a submersible vessel using CFD software, while in [15], the motion of submerged submarines was analysed under lateral wave impacts. The study in [16] investigated the motion of submerged bodies near liquid surfaces and under ice, and revealed the impact of ice thickness on wave resistance and lift force. In [17], a dynamic overset methodology was introduced to analyse the response of BB2 geometry during self-propulsion near the free surface. While this research aimed to analyse the impact of wave disturbance on fluid dynamic shapes optimised for underwater operation, with a focus on enhancing wave-following characteristics and motion stability near the water surface.

Research in the area of wave glider collision avoidance involves developing obstacle avoidance algorithms, including global and local path planning methods. Autonomous algorithms that leverage machine learning and artificial intelligence can process real-time sensor data to identify hazards and generate evasive actions. The authors of [18] summarised existing AI-based surface collision avoidance methods, while in [19], a speed-adaptive robust obstacle avoidance approach was proposed using deep reinforcement learning. In [20], an obstacle avoidance fusion algorithm was introduced to overcome the dynamic challenges posed by limited wave glider manoeuvrability.

Despite these efforts, achieving proficient collision avoidance through path planning and control algorithms represents a formidable obstacle. In particular, wave gliders struggle to avert collisions with swiftly approaching surface vessels or trawling fishing vessels. During sea trials of a conventional wave glider, we encountered multiple instances of damage resulting from entanglement with fishing nets, as depicted in Fig. 1, which shows impairment to a wave glider's steering apparatus and umbilical cable due to interaction with a fishing net.

Fig. 1. Damage to the rudder and umbilical cable of a wave glider caused by fishing nets

Wave gliders remain susceptible to active damage due to their weak manoeuvrability and inability to dive. Their endurance is largely dependent on whether they are artificially damaged, rather than the reliability of the system itself. Hence, there is a significant need for innovations in wave glider technology to improve collision avoidance safety. The idea underlying this study is to exploit the good concealment and buoyancy control technology of a semi-submersible vehicle, which allows it to dive, to improve collision avoidance safety.

Semi-submersible vehicles are characterised by a main structure that is submerged underwater with minimal surface exposure, thereby enhancing their stealth capabilities. This submerged design also contributes to increased stability in a wave environment compared to surface vehicles [21]. In addition, semi-submersible vehicles have the ability to dive and float by adjusting their buoyancy, a feature that greatly enhances their safety and survivability in rough sea conditions and allows for effective collision avoidance. Buoyancy regulation technology has been used extensively in marine robotics, for example in underwater gliders [22].

The integration of semi-submersible vehicle technics into wave-propelled unmanned vehicles offers a compelling opportunity to enhance their capabilities. Submersible and semi-submersible vehicles possess intrinsic advantages in terms of stealth and safety, making them an ideal platform for unmanned marine operations. By harnessing these advantages, wave-propelled unmanned vehicles can achieve improved collision avoidance and overall safety. This study explores novel approaches to incorporating the benefits of submersible semi-submersible vehicles and buoyancy regulation technology into wave-propelled unmanned vehicles, with the aim of advancing the field of marine robotics and facilitating safer and more efficient marine operations. The aims of this article are to introduce an innovative vehicle concept,

to evaluate the feasibility of its foundational principles, and to acquire preliminary navigation performance parameters for the proposed system. The main contributions of this paper are the proposal of a novel semi-submersible wave-propelled unmanned vehicle and validation of the feasibility of the design solution through modelling, simulation, and testing the prototype of WPSUV in laboratory and at-sea.

The rest of this paper is organised as follows: Section II introduces the general scheme for the proposed wave-propelled unmanned surface vehicle (WPSUV), Section III explains the modelling of the WPSUV's dynamics, Section IV describes the simulations of the WPSUV, which were carried out to obtain the kinematic performance of the system under various sea conditions, Section V details the laboratory tests and the sea trials conducted on the WPSUV, Section VI presents some results and a discussion of this research, and Section VII presents the conclusions of the study and discusses potential directions for future research.

DESIGN OF THE WPSUV

OVERALL SCHEME OF THE WPSUV

The proposed WPSUV has a two-body design similar to that of a wave glider, consisting of a float (navigation body) and a submerged glider coupled with a flexible umbilical cable. With six pairs of hydrofoils on the submerged glider, the WPSUV uses the core operating concept of a wave glider to transform the platform's heave motion into forward thrust. Steering control force is provided by the rudder, and auxiliary propulsion is used to combat ocean currents when necessary. Fig. 2 shows a 3D rendering of the overall scheme of the WPSUV.

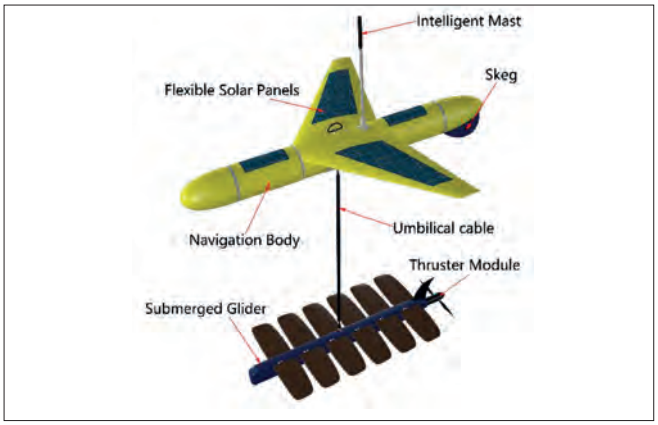

Fig. 2. 3D rendering of the overall scheme for the WPSUV

The main innovation of our WPSUV is the design of a navigation body with a high lift-to-drag ratio to replace the float of a wave glider. Compared with the positive buoyancy of the wave glider, our WPSUV is configured with micro-positive buoyancy. The lift provided by the navigation body generates good wave-following motion, which helps the vehicle capture wave kinetic energy. This allows the WPSUV to achieve higher speeds and greater manoeuvrability than traditional wave gliders.

A variable-chord swept-back wing with a NACA4412 airfoil section is attached to the streamlined body, and provides lift during navigation. The wing gives the system good drag performance, while the large wingspan creates a large drag surface when undulating with the waves, allowing the system to maximise the capture of wave kinetic energy in a near-zero buoyancy configuration.

The main part of the navigational body, which consists of a curved head section, a cylindrical middle section, and a curved tail section, adopts the streamlined shape of the rotating body. The middle section of the navigational body is designed with a pressure-resistant seal to provide mounting space for non-watertight components. A set of buoyancy adjustment devices is mounted inside the body to allow the buoyancy of the vehicle to be quickly adjusted for diving and floating.

The intelligent mast system, which is mounted above the body and integrates sound, light, short-wave, satellite, automatic identification system (AIS) and other sensors with communication and alert functions, is capable of long-distance communication with space-based, ship-based and shore-based communication equipment. It can also autonomously identify surface targets for alerts.

In the event that a dangerous target is approaching or there are extreme sea conditions, the buoyancy regulation system can implement an avoidance dive. Heading stability is provided by the tail wing, which is mounted below aft.

Flexible solar panels that provide additional electricity for the vehicle's task sensors and control system are installed on the upper surface of the navigation body. The solar panels can operate effectively when the upper surface of the navigation body is out of the water by adjusting buoyancy.

The main performance parameters of WPSUV are shown in Table 1.

Tab. 1. Main parameters of the WPSUV

Parameter	Value
Weight	150.0 kg
Float dimensions	φ 300.0 mm × 3.0 m
Wing span	2.4 m
Submerged glider dimensions	1.9 × 1.1 × 0.4 m
Umbilical length	6.0 m
Buoyancy capacity	30 l
Maximum diving depth	100.0 m

BUOYANCY REGULATION SYSTEM DESIGN

To avoid collisions and rough seas, a buoyancy regulation system is employed. There are three main methods for changing a vehicle's buoyancy, based on the use of ballast tanks, high-pressure air, and hydraulic oil bladders. The necessity for rapidity and large displacement led to a decision to use a ballast water tank for this vehicle. The vehicle is equipped with a pressure-resistant water tank whose volume is equal to the required maximum buoyancy adjustment. When the buoyancy needs to be changed, the water in the pressure-resistant tank is either injected from the

ocean or evacuated by a volumetric seawater pump, thus changing the craft's weight and adjusting its ability to sink or float. The initial internal pressure of the ballast tank is designed to be in a negative pressure state of less than one atmosphere. To mitigate the impact of wing resistance during diving, the water tank is located at the head of the vehicle. Upon entry of seawater, the vehicle's posture undergoes a transformation, enabling a smooth and rapid descent. This approach eliminates the problems related to a skin bag, simplifies the system, decreases weight and space, and concurrently boosts the system reliability and the vehicle's dive speed. Fig. 3 shows a schematic diagram of the buoyancy regulation system.

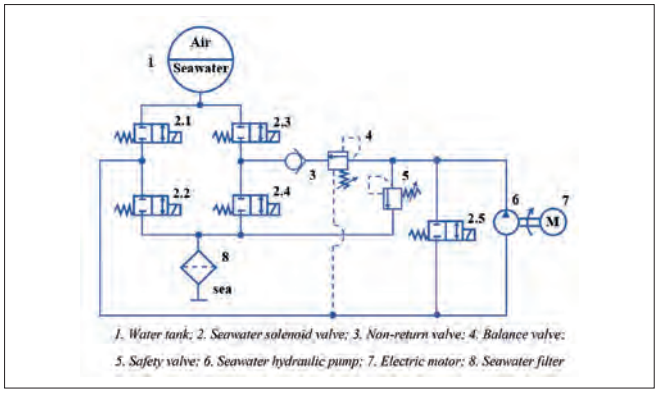

Fig. 3. Diagram of showing the principle of the buoyancy regulation system

The main component of the buoyancy regulation system is a seawater pump, which rapidly lowers or raises the vehicle by drawing in and releasing seawater. When the vehicle needs to dive urgently, the buoyancy regulation system activates the suction mode upon receiving the command. Seawater is quickly sucked into the ballast water tank, thus enabling the vehicle to dive quickly to a specific depth below the surface. By adjusting the suction speed and the time taken for valve closure, the system's dive speed and depth can be controlled. The drainage mode is turned on, and the water in the ballast tank is released to raise the vehicle to the surface after the system has stabilised at a specific depth for a predetermined amount of time (which can be set).

In the sealed cabin, pumping equipment consisting of a seawater pump, bracket, elastic coupling, and DC motor is mounted. The seawater solenoid valve is installed in the cabin in contact with sea water, and a seawater filter is installed at the inlet of the seawater solenoid valve. Several pipeline accessories connect the functional modules together. Fig. 4 shows the partial structure of the buoyancy regulation system module.

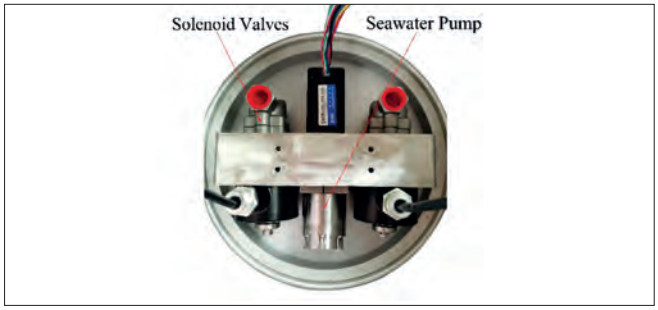

Fig. 4. Buoyancy regulation system module

DYNAMIC MODELLING AND MOTION SIMULATION OF THE WPSUV

DEFINITION OF THE COORDINATE SYSTEM

The body coordinate system for the navigating body is defined with its origin at the centre of buoyancy. The x-axis extends forward along the major axis, while the y-axis lies in the longitudinal plane, pointing upward perpendicular to the x-axis. The z-axis completes the right-handed coordinate system, lying perpendicular to both the x-axis and y-axis.

Similarly, the body coordinate system for the submerged glider has its origin at the centre of floatation. The x-axis points forward along the longitudinal axis, and the y-axis lies in the longitudinal plane, pointing upward perpendicular to the x-axis. The z-axis is oriented perpendicular to the x- and y-axes, completing the right-handed coordinate system.

Fig. 5 illustrates the coordinate systems for both the navigating body and the submerged glider.

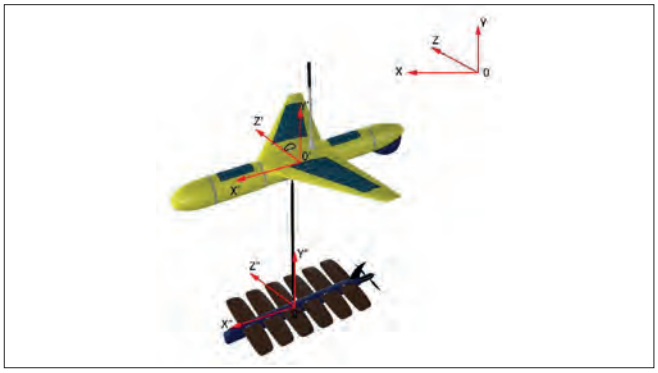

Fig. 5. Coordinate systems used for the WPSUV

NONLINEAR 6DOF RIGID-BODY EQUATIONS OF MOTION

In dynamic modelling, the vehicle is considered as a multi-body system composed of multiple rigid bodies, including the navigating body, umbilical cable, submerged glider, and flapping foils. The umbilical cable is a flexible structure, but to simplify the calculation, it is approximated as a multi-segment rigid structure. The matrix form of the dynamic equation for each rigid body is:

$$m\frac{dv}{dt} = F = [F_x \;\; F_y \;\; F_z]^{\mathrm{T}} \tag{1}$$

$$\frac{dK}{dt} = M = [M_x \;\; M_y \;\; M_z]^{\mathrm{T}} \tag{2}$$

where m is the mass of the rigid body, v is the velocity vector, K is the total momentum moment, F is the combined external force, and M is the combined external moment. All forces and moments are defined at the centre of mass of the rigid body.

The matrix form of the equation can be expressed as [23]:

$$M_{\mathrm{RB}}\dot{V} + C_{\mathrm{RB}}(V)V = \tau \tag{3}$$

where M_{RB} is the matrix of inertia coefficients, $C_{RB}(V)$ is the Coriolis centripetal force matrix, and $\tau = [F \ M]^T$.

The vector expression for the kinematic equation is:

$$\dot{P} = J(\varphi, \psi, \theta)V \tag{4}$$

where

- $P = [x, y, z, \varphi, \psi, \theta]^T$ is the generalised coordinate vector
- $V = [v_x, v_y, v_z, \omega_x, \omega_y, \omega_z]^T$ is the generalised velocity vector
- $J(\varphi, \psi, \theta) = \begin{bmatrix} R_E^B & O_{3\times3} \\ O_{3\times3} & T^{-1} \end{bmatrix}$ is the kinematic Jacobi matrix

and R_E^B is the transformation matrix from the body coordinate system to the geodetic coordinate system. We also have

$$T^{-1} = \begin{bmatrix} 1 & -\tan\theta\cos\varphi & \tan\theta\sin\varphi \\ 0 & \sec\theta\cos\varphi & -\sec\theta\sin\varphi \\ 0 & \sin\varphi & \cos\varphi \end{bmatrix} \tag{5}$$

WAVE FORCE CALCULATION MODEL AND NUMERICAL SOLUTION

Using a binary cosine wave model, the velocity potential of the incident wave is expressed as:

$$\Phi' = Ae^B\phi_0 \tag{6}$$

where

$$B = ky_0 + i(\omega t + \varepsilon_0 - kx_0\cos\gamma - kz_0\sin\gamma) \tag{7}$$

$$\phi_0 = \frac{ig}{\omega}\exp\{k(x\sin\theta + y\cos\theta\cos\varphi - z\cos\theta\sin\varphi - H) - ik\cos\gamma[x\cos\theta\cos\psi + y(\sin\psi\sin\varphi - \sin\theta\cos\psi\cos\varphi) + z(\sin\psi\cos\varphi + \sin\theta\cos\psi\sin\varphi)] - ik\sin\gamma[-x\cos\theta\sin\psi + y(\cos\psi\sin\varphi + \sin\theta\sin\psi\cos\varphi) + z(\cos\psi\cos\varphi - \sin\theta\sin\psi\sin\varphi)]\} \tag{8}$$

where A is the wave amplitude, k is the wave number, and ω is the angular frequency. H is the distance of the geodesic origin from the still water surface, which is positive when the origin is underwater, and γ is the wave direction angle.

When the vehicle moves through waves, the waves have a perturbing effect on the vehicle and the vehicle scatters the waves, resulting in a diffractive flow field. The diffraction potential is:

$$\Phi'' = Ae^B\phi_7 \tag{9}$$

The relationship between ϕ_7 and ϕ_1 is:

$$\left.\frac{\partial\phi_7}{\partial\vec{n}}\right|_{S_b} = -\left.\frac{\partial\phi_0}{\partial\vec{n}}\right|_{S_b} \tag{10}$$

where S_b is the wetted surface area of the vehicle, and $\vec{n}$ is the unit outer normal vector of the surface of the vehicle.

Thus, the wave-generated disturbed flow field is:

$$\Phi = \Phi' + \Phi'' = Ae^B(\phi_7 + \phi_0) \tag{11}$$

The wave-generated disturbed pressure field is:

$$p = -\rho\mathrm{Re}\left(\frac{\partial\Phi}{\partial t} - v\cdot\nabla\Phi\right) \tag{12}$$

Since $\dot{x}_0 = v_{x0}$, $\dot{y}_0 = y_{x0}$, $\dot{z}_0 = z_{x0}$, the formula can be rearranged as:

$$p = -\rho\mathrm{Re}i\omega Ae^B(\phi_0 + \phi_7) \tag{13}$$

Integrating the pressure p over the wetted surface area S_b of the vehicle gives the wave disturbance force F_w and disturbance moment M_w:

$$\vec{F}_w = -\iint_{S_b} p\vec{n}\,dS \tag{14}$$

$$\vec{M}_w = -\iint_{S_b} p\vec{r}\times\vec{n}\,dS \tag{15}$$

CONSTRUCTION OF THE SIMULATION MODEL

A near-surface motion model of the WPSUV was constructed using the Modelica language and simulated under the multidisciplinary simulation platform OpenModelica 1.21.0. A block diagram of the model is shown in Fig. 6, where:

- **Wave:** Wave force module
- **Navigation body:** Six-degree-of-freedom (6DOF) motion module of the near-surface platform
- **Cable:** Umbilical motion module
- **Glider frame:** 6DOF motion module of the submerged glider frame
- **Fin:** 6DOF motion module of a pair of flapping foils

The navigation body module outputs the displacement and attitude to the wave module. the wave module calculates the wave force on the platform based on the displacement and attitude of the platform near the water surface and outputs it to the navigation body module. L1 to L11 are structural size models, and r1 and r2 are hinge models.

This modular approach enables the individual components of the WPSUV to be modelled and simulated independently, which facilitates the development and optimisation of the overall system.

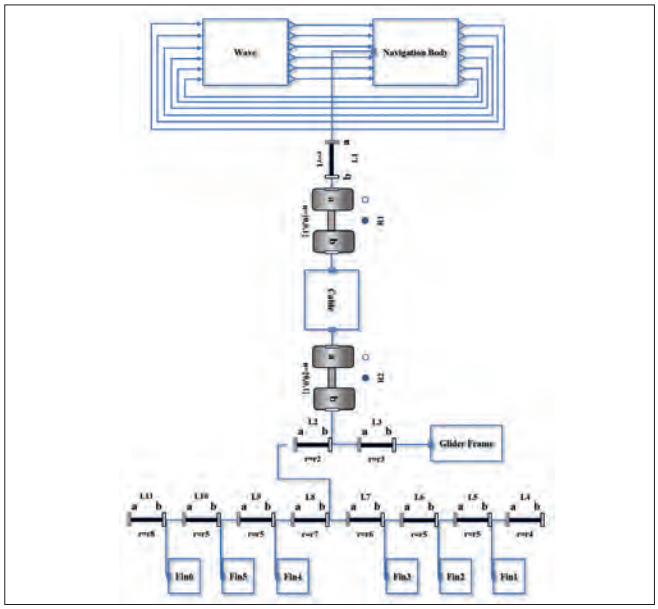

Fig. 6. Motion model of the WPSUV near the water surface

The umbilical cable is modelled using a finite segment approach, in which it is divided into five segments over the cable length (chosen based on the calculation volume and calculation accuracy). A sub-model block diagram is shown in Fig. 7, where:

- **Sec:** Single-segment cable 6DOF model

The segments are connected by hinges, which allows for realistic simulation of the flexibility and dynamics of the umbilical cable.

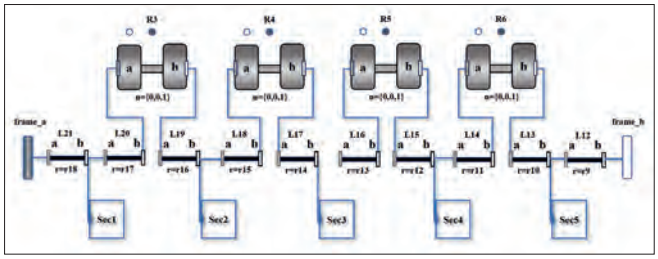

Fig. 7. Umbilical sub-module

The Fin sub-model is shown in Fig. 8, where:

- **Fin_6dof_mod:** 6DOF motion model of the flapping foil containing hydrodynamic forces

The Fin_6dof_mod is connected to the glider frame sub-model via hinges, with damping and limiting. This configuration allows the fins to flap freely while also limiting their range of motion to prevent damage or excessive strain, thus ensuring optimal wave kinetic energy conversion. The hydrodynamic forces acting on the fins are calculated based on their motion and the surrounding fluid flow, enabling realistic simulation of their propulsive and manoeuvring capabilities.

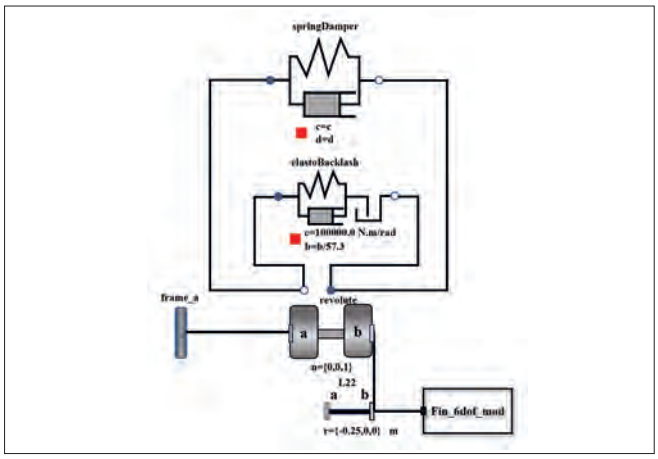

Fig. 8. Fin submodule

LABORATORY TEST AND SEA TRIALS

LABORATORY TESTS

Laboratory testing was conducted in three parts: communication and control system testing, buoyancy regulation system testing, and weight configuration and attitude testing.

Communication and Control System Testing

The communication and control system is designed to be similar to that of a traditional wave glider. It consists of a wireless and satellite communication system that sends commands for external equipment control, route planning, equipment status monitoring, and parameter setting. The control system includes internal data control and motion control. The basic performance and connectivity tests of this system were completed in the laboratory (see Fig. 9).

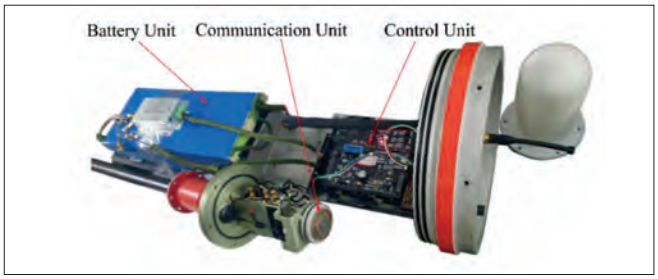

Fig. 9. Laboratory testing of the communication and control system

Buoyancy Regulation System Testing

The buoyancy regulation system is designed as a separate compartment for precise and quantitative intake or discharge of seawater. The system is designed for a maximum intake and discharge volume of 20 l of seawater, which corresponds to the volume of the tank to which it is connected. The water absorption rate is greater than 100 l min^{-1}, and the drainage rate is greater than 1 l min^{-1}. Due to the high timeliness requirements for vehicle dives and low timeliness standards for uplifts, the water intake rate is significantly higher than the water release rate. During the test, the entire buoyancy regulator assembly was submerged in water, the inhalation or exhalation mode was activated, and the amount of seawater inhaled or exhaled was timed and measured (see Fig. 10).

Fig.10. Test of buoyancy regulation system module

Pool Weighing Configuration and Attitude Testing

Tests of the weight configuration and attitude of the WPSUV prototype were conducted in a test tank. These experiments were carried out to obtain the attitude of the navigation body and submerged glider under various buoyancy configurations, and to determine the maximum amount of buoyancy adjustment required. When the vehicle was configured for micro-positive buoyancy, the maximum weight that could be carried was more than 60 kg. The limited depth of the pool prevented testing for diving and floating, which were planned to be carried out at sea. The WPSUV prototype is shown in the pool in Fig. 11.

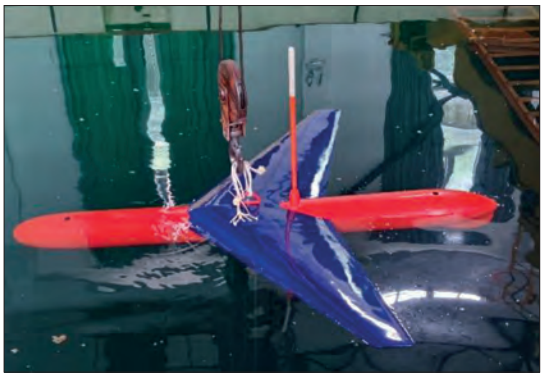

Fig. 11. Pool-based weighing configuration and attitude test of the WPSUV prototype

SEA TRIAL

The main purpose of the sea trial was to verify the feasibility of the kinematic principle of the WPSUV. Hence, the prototype did not have full functionality. The WPSUV sea trial prototype is shown in Fig. 12. Compared to the full conceptual design of the WPSUV, the test prototype excluded some non-essential functional components:

- The submerged glider (including the rudder) and the umbilical cable were taken from existing prototypes of conventional wave gliders.
- The smart mast did not have an independent surface ship detection capability, and was only used for communications.
- The underwater glider was not equipped with thrusters.
- The prototype lacked flexible solar panels.

Fig. 12. The WPSUV sea trial prototype

Navigation testing

Navigation tests were conducted based on straight-line round-trip navigation and route tracking navigation. Two sea trials were executed: one within Zhanjiang Harbour, and the other outside the harbour. During the first sea trial (conducted within Zhanjiang Harbor), sea conditions were tranquil, with visually measured wave heights of below 20 cm. The second sea trial was conducted off the port of Zhanjiang under low sea conditions, with a maximum visually measured wave height of less than 50 cm. Fig. 13 illustrates the sea trial area and the WPSUV's sailing status.

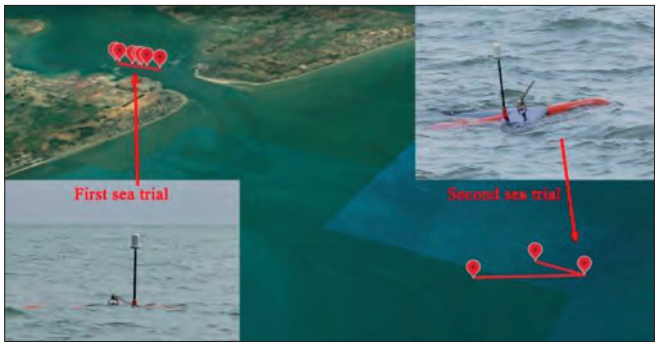

Fig. 13. Sea trial area and sailing status of the WPSUV

Diving and Floating Tests

During this sea trial, comprehensive testing of the vehicle's diving speed, depth, flow control, and other parameters was deferred, as the system was in an early developmental stage. Instead, the focus was on validating the vehicle's surfacing and diving capabilities. The ability to rapidly adjust the buoyancy of the vehicle was assessed through controlled opening and closing of the solenoid valve and seawater pump. To safeguard the prototype, a tether was employed to tow the submerged glider during testing. Fig. 14 illustrates the diving process of the WPSUV.

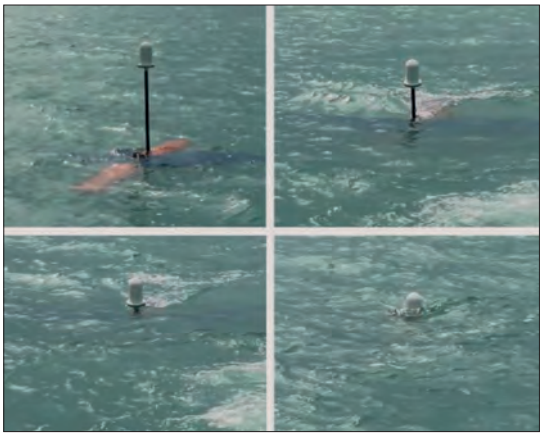

Fig. 14. Diving process of the WPSUV

RESULTS AND DISCUSSION

Despite the sea trial prototype deviating slightly from the design specifications, and the lack of precise measurements of sea state parameters such as waves and currents, the test data provided valuable insights into the WPSUV's performance

under real-world conditions. According to the results of the theoretical model simulation and the experimental data, the proposed WPSUV has significant advantages in terms of collision avoidance safety, load capacity and sea state adaptability compared with traditional wave gliders.

COLLISION AVOIDANCE VERSUS SECURITY AND CONCEALMENT

The WPSUV's micro-positive buoyancy configuration submerges its main structure, reducing its visual signature on the surface. This reduced visibility makes the WPSUV less likely to be detected and collided with by other vessels, enhancing its stealth capability. By adjusting its buoyancy, the WPSUV can achieve multiple modes of motion, including surface, near-surface and underwater (as shown in Fig. 15). This multi-mode capability provides the WPSUV with greater flexibility and manoeuvrability in varying sea conditions. In addition, the ability to switch between different modes of movement enhances the WPSUV's collision avoidance capabilities.

The WPSUV's unique combination of stealth capabilities and multi-mode movement makes it well suited to a wide range of applications, including marine environmental protection, resource exploration and the protection of maritime interests.

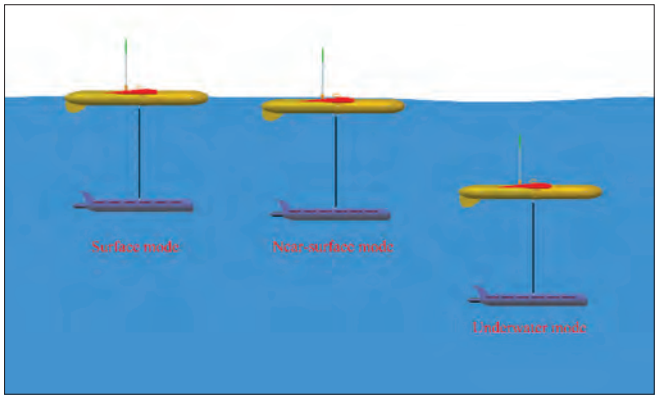

Fig. 15. Schematic of WPSUV multi-mode motion

EFFECT OF SEA STATE ON NAVIGATION PERFORMANCE AND MOTION STABILITY

To investigate the navigational performance and motion stability, system motion simulations and prototype sea trials were carried out. The main objective of the simulations was to obtain the performance parameters, such as speed and attitude stability, of the WPSUV under different sea states. The WPSUV has various navigation modes, including surface mode, underwater mode and semi-submersible mode with exposed communication antenna. These simulations focused on the semi-submersible mode.

Simulation conditions were designed to represent four different sea states: a calm sea state (Case 1), moderate sea states (Cases 2 and 3), and a high sea state (Case 4). The wave parameters for each simulation condition are summarised in Table 2.

Tab. 2. Wave parameters for various simulation conditions

Simulation case	Wave amplitude	Wave period	Wavelength
1	0.5 m	3 s	14.051 m
2	1.0 m	4 s	24.981 m
3	2.0 m	6 s	56.207 m
4	8.0 m	12 s	224.8 m

The wave amplitude and period were directly selected based on typical sea state data. The wavelength was then determined using the following relationship:

$$\lambda = \frac{\tau^2 g}{2\pi} \tag{21}$$

where:

- λ is the wavelength
- g is the acceleration due to gravity
- τ is the wave period

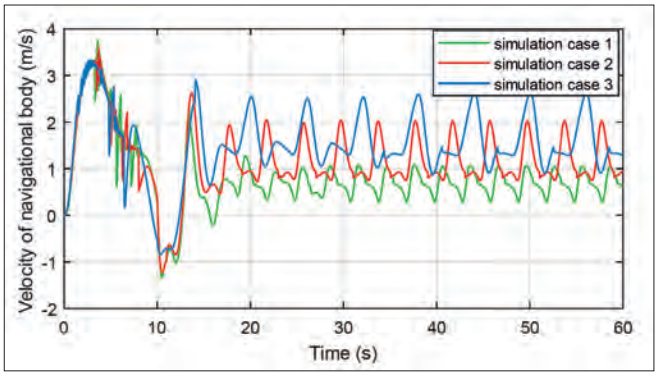

Fig. 16. Velocity of navigational body under different simulation cases

Fig. 16 shows the velocity variations of the navigating body under different simulation scenarios. The initial phase of the velocity profile corresponds to the launch process, which is characterised by an unsTable 2 state. Following stabilisation, the WPSUV achieved velocities of 0.68, 1.19, and 1.59 m s-1, respectively.

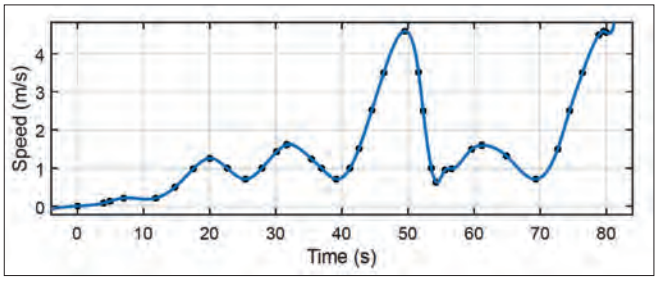

Fig. 17. Speed of the WPSUV over time under extreme sea conditions

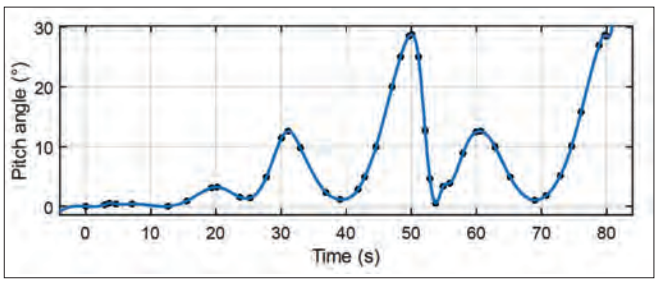

Fig. 18. Pitch angle over time for the WPSUV under extreme sea conditions

Figs. 17 and 18 show the velocity and pitch angle of the WPSUV under extreme sea conditions (Case 4). The results reveal a substantial decrease in the vehicle's stability in rough sea states. The velocity and pitch angle exhibit increased erratic behaviour, indicating that the WPSUV encounters challenges in terms of maintaining a sTable 2 attitude amidst high waves.

The simulation findings demonstrate the WPSUV's capability to operate across a wide range of sea states, encompassing extreme conditions. Nonetheless, in high sea conditions, the WPSUV's stability may be compromised. Consequently, it is imperative to consider motion mode switching, such as diving, to ensure the WPSUV's survivability in rough sea conditions.

While high sea states may decrease the system's motion stability due to weak positive buoyancy, extreme sea states can be effectively avoided by submerging the WPSUV. This submergence capability makes the proposed WPSUV more adapTable 2 to sea states than conventional wave gliders.

From the sea trial results, we observed that the planned route for the first test approximated a straight line, resulting in minimal deviation of the actual trajectory from the intended path. The maximum vertical deviation from the planned route was approximately 144 m, with an average deviation of less than 50 m, representing good path tracking performance. The average speed during the first test was 0.34 m/s. Fig. 19 depicts the planned routes and actual trajectories, while Fig. 20 shows the actual speed profile for the WPSUV.

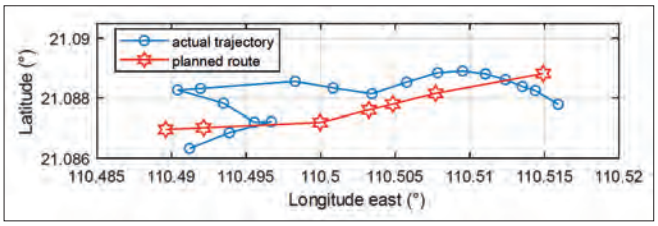

Fig. 19. Results for the first sea trial: planned routes and actual trajectories

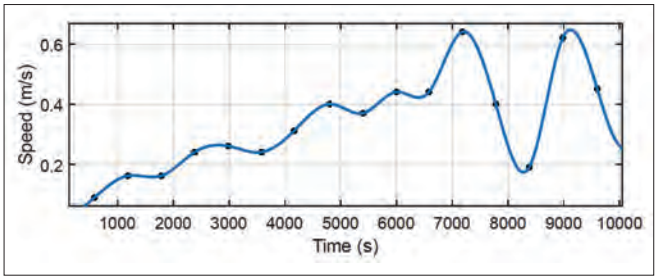

Fig. 20. Results for the first sea trial: sailing speed of the WPSUV

The initial plan for the second sea trial was to follow a straight course; however, during the voyage, the vehicle encountered sea currents that caused significant deviation from the intended path. The speed of the current was not measured during the sea trial, but was roughly estimated as flowing in a south-westerly direction. Consequently, the planned route was temporarily modified to align with the current's flow direction. Throughout the test, the vehicle experienced both countercurrent and forward flow conditions. Fig. 21 depicts the planned routes and actual trajectories, while Fig. 22 shows the speed profile of the WPSUV. The average speed during the second test was 0.36 m s^{-1}.

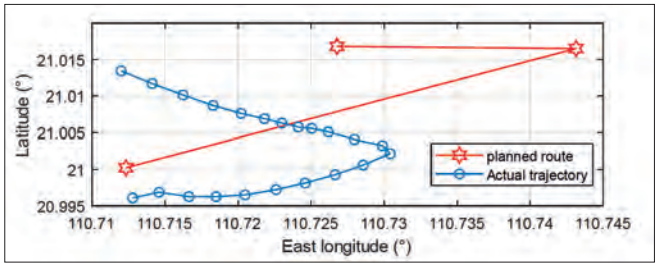

Fig. 21. Results of the second test: planned routes and actual trajectories

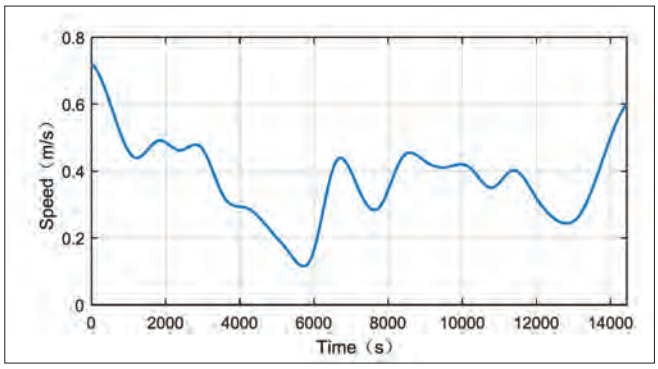

Fig. 22. Results of the second sea trial: sailing speed of the WPSUV

During the second sea trial, a noTable 2discrepancy was observed between the actual trajectory of the vehicle and the planned route. This deviation can be attributed to the fact that the vehicle relies entirely on wave energy as its sole source of kinetic energy. When the power generated by the waves falls short of meeting the demands posed by the current, the vehicle inevitably veers off course. Consequently, auxiliary propulsion remains essential in areas characterised by calm sea conditions and significant current effects.

Based on the observed sea conditions, the previously established dynamic model was utilised to simulate the vehicle's performance under wave amplitudes of 0.25 m and 0.35 m. The simulation results revealed average velocities after system stabilisation of 0.243 m s^{-1} and 0.4 m s^{-1}, respectively, as shown in Fig. 23. The close match between the simulated and measured velocities serves as validation of the model's effectiveness. Nevertheless, due to incomplete knowledge of the sea conditions and the factors influencing the vehicle's navigation performance, further in-depth research is required to refine the dynamic simulation model, and actual navigation testing of the vehicle should be conducted.

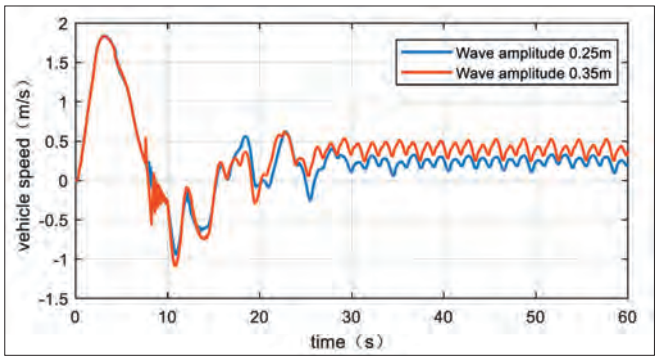

Fig. 23. Simulation results: vehicle speed under wave amplitudes of 0.25 m and 0.35 m

The sea trial results indicate that the WPSUV's high lift-to-drag ratio navigation body and reduced system drag enable it to achieve good speeds in calm and moderate sea conditions. Coupled with the diminished influence of wind due to the WPSUV's subsurface operation, this may enhance its position control performance under the influence of currents. The findings of the system motion simulation and sea navigation test collectively demonstrate the exceptional navigation performance of the proposed WPSUV and its adaptability to varying sea conditions.

DIVING PROMPTNESS OF THE WPSUV

The WPSUV employs a seawater pump buoyancy regulation system, which enables it to intake or discharge seawater, thereby inducing changes in buoyancy and attitude. This enables the vehicle to perform diving and floating movements, allowing it to avoid hazardous targets and extreme sea conditions and enhancing its safety. Specifically, when avoiding dangerous targets such as fast-approaching surface vessels, the diving speed must be optimised to reach a safe depth quickly, in order to ensure the vehicle's safe operation.

During the diving process, the buoyancy regulating system must first take in water, followed by drainage after reaching a certain diving speed and depth, and the vehicle finally stabilises at a safe depth. This dynamic process is exemplified in Fig. 24, which presents the simulation results for the vehicle's depth, water volume, and pitch angle during a dive, specifically for a maximum dive depth of less than 50 m.

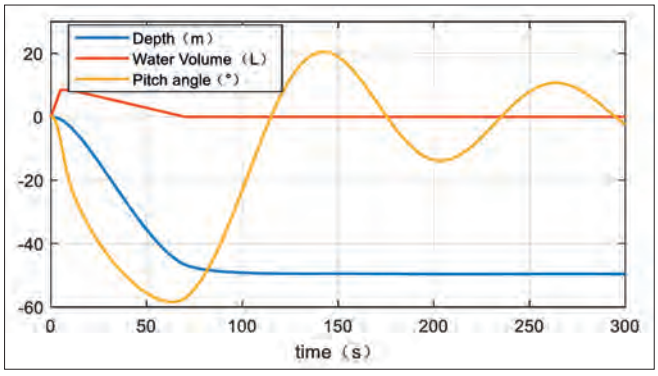

Fig. 24. Diving process of WPSUV

The ballast tank of the buoyancy regulation system is located at the head of the vehicle, allowing for a gradual increase in negative buoyancy following the initial stage of the dive as seawater is taken in. This change in buoyancy is accompanied by a shift in the pitch attitude, which in turn reduces the resistance experienced during the dive. During the subsequent drainage phase, the pitch attitude is simultaneously adjusted, ultimately reaching an equilibrium state. It can be seen that the water intake reaches 8.5 l, and the dive depth of the vehicle within 10 s is about 3 m. Based on the assumption that a surface vessel is approaching at a distance of 100 m and a speed of 10 m per second, the vehicle dives to a depth of approximately 3 m before the surface vessel arrives. This depth is deemed sufficient to ensure the safety of the vehicle, as adjustments in buoyancy facilitate a more rapid descent of the vehicle.

EFFECT ON VEHICLE LOAD CAPACITY OF THE SEMI-SUBMERSIBLE DESIGN

The innovative wave propulsion system of the proposed WPSUV eliminates the reliance on substantial positive buoyancy for locomotion. This buoyancy can be reallocated to payload capacity, resulting in a significant increase compared to traditional wave gliders. The prototype WPSUV boasts a maximum payload capacity of approximately 60 kg, representing a 30% enhancement over conventional wave gliders. For instance, the SV3 wave glider from Liquid Robotics has a maximum payload capacity of 45 kg [24]. This increase in payload capacity will make it possible to carry more sensors for different missions.

CONCLUSION AND FUTURE WORK

This paper has proposed an innovative WPSUV and has verified the feasibility of its principle through modelling, simulation, prototype design, and testing. Sea navigation test data demonstrate that our WPSUV is capable of achieving high speeds and motion stability in low sea states. Furthermore, the vehicle's ability to dive rapidly through buoyancy adjustment means that it is effective in avoiding collisions. The principle of motion of the WPSUV represents a new concept for unmanned vehicles, with enhanced collision avoidance safety and increased payload capacity for extended missions.

The key findings of this study are that the proposed WPSUV has enhanced collision avoidance capabilities by diving, and that the principle underlying this novel vehicle design is feasible. Specifically, the use of a slightly positively buoyant vehicle with a high lift-to-drag ratio rather than a traditional positively buoyant boat can yield favourable wave-following characteristics, and can effectively harness wave kinetic energy.

This study primarily focused on verifying the feasibility of the principle of operation of the WPSUV, and it is important to acknowledge that the functionality of the prototype is not yet complete. The motion simulation and performance testing of the system remain insufficient. The aim of future work should be to optimise the dynamic model of the WPSUV, taking into account nonlinear wave loads in real marine environments. Important next steps will include establishing a dynamic motion model for the underwater vehicle with variable buoyancy and conducting simulation and experimental research to obtain control parameters for diving and floating. In addition, comprehensive navigation performance tests should be conducted, including testing of performance under high sea conditions and long-term motion reliability in the marine environment. Based on the simulation and test results, further optimisation of the vehicle can be carried out.

In summary, this study lays the foundation for the development of the proposed WPSUV and highlights the importance of future research efforts to enhance its functionality, performance, and reliability. When the areas identified for improvement have been addressed and additional testing and optimisation have been conducted, the proposed

WPSUV will offer great potential as an advanced unmanned vehicle with superior collision avoidance capabilities in marine environments.

REFERENCES

1. Palmer MR et al. Marine robots for coastal ocean research in the Western Indian Ocean. Ocean & Coastal Management 2021, 212, 105805. https://doi.org/10.1016/j.ocecoaman.2021.105805

2. Tian B, Guo J, Song Y, Zhou Y, Xu Z, Wang L. Research progress and prospects of gliding robots applied in ocean observation. Journal of Ocean Engineering and Marine Energy 2023, 9(1), 113-124. https://doi.org/10.1007/S40722-022-00247-W

3. Zereik E, Bibuli M, Mišković N, Ridao P, Pascoal A. Challenges and future trends in marine robotics. Annual Reviews in Control 2018, 46, 350-368. https://doi.org/10.1016/j.arcontrol.2018.10.002

4. Wang L, Li H. Dynamics and power performance of a novel wave-powered unmanned surface vehicle. Marine Structures 2024, 93, 103543. https://doi.org/10.1016/j.marstruc.2023.103543

5. Daniel T, Manley J, Trenaman N. The wave glider: Enabling a new approach to persistent ocean observation and research. Ocean Dynamics 2011, 61(10), 1509-1520. https://doi.org/10.1007/S10236-011-0408-5

6. Schmidt KM et al. Evaluation of satellite and reanalysis wind products with in situ wave glider wind observations in the Southern Ocean. Journal of Atmospheric & Oceanic Technology, 2017, 34(12), 2551-2568: JTECH-D-17-0079.1. https://doi.org/10.1175/jtech-d-17-0079.1

7. Thomson J et al. Measurements of directional wave spectra and wind stress from a wave glider autonomous surface vehicle. Journal of Atmospheric and Oceanic Technology, 2018, (35)2, 347-363: jtech-d-17-0091.1. https://doi.org/10.1175/jtech-d-17-0091.1

8. Amiruddin, MS. Real-time Web GIS to monitor marine water quality using wave glider. IOP Conference Series: Earth and Environmental Science, 2016:012074. https://doi.org/10.1088/1755-1315/37/1/012074

9. Foster JH, Ericksen TL, Bingham B. Wave-glider-enhanced vertical seafloor geodesy. Journal of Atmospheric and Oceanic Technology 2020, 37(3), 417-427. https://doi.org/10.1175/jtech-d-19-0095.1

10. Anderson EE et al. Summer diatom blooms in the eastern North Pacific gyre investigated with a long-endurance autonomous surface vehicle. PeerJ, 2018, 6: e5387. https://doi.org/10.7717/peerj.5387

11. Zhang Y, Kieft B, Rueda C, O'Reilly T, Chavez F. Autonomous front tracking by a wave glider. Oceans 2016, 1-4. https://doi.org/10.1109/oceans.2016.7761070

12. Chérubin LM et al. Fish spawning aggregations dynamics as inferred from a novel, persistent presence robotic approach. Frontiers in Marine Science 2020, 6, 779. https://doi.org/10.3389/fmars.2019.00779

13. Lan H et al. Acoustical observation with multiple wave gliders for internet of underwater things. IEEE Internet of Things Journal 2020, 8(4): 2814-2825. https://doi.org/10.1109/jiot.2020.3020862

14. Yoon GH, Seo JW, Yoon HK. Dynamic control of an underwater vehicle near wave surface. Oceans 2018, MTS/IEEE Charleston, Charleston, SC, USA, 2018, pp. 1-7. https://doi.org/10.1109/oceans.2018.8604778

15. Gaafary MM. Motion of submerged submarine in the near surface lateral waves. Port-Said Engineering Research Journal 2021, 25(1), 66-74. https://doi.org/10.21608/pserj.2020.31103.1041

16. Zemlyak V, Pogorelova A, Kozin V. Motion of a submerged body in a near-surface water environment. International Journal of Naval Architecture and Ocean Engineering 2022, 14, 100433. https://doi.org/10.1016/j.ijnaoe.2021.100433

17. Carrica PM, Kim Y, Ezequiel Martin J. Near-surface self propulsion of a generic submarine in calm water and waves. Ocean Engineering 2019, 183, 87-105. https://doi.org/10.1016/j.oceaneng.2019.04.082

18. Burmeister H-C, Constapel M. Autonomous collision avoidance at sea: A survey. Frontiers in Robotics and AI 8, 2021, p. 739013. https://doi.org/10.3389/frobt.2021.739013

19. Wang P et al. Obstacle avoidance for environmentally-driven USVs based on deep reinforcement learning in large-scale uncertain environments. Ocean Engineering 2023, 270, 113670. https://doi.org/10.1016/j.oceaneng.2023.113670

20. Wang D et al. An obstacle avoidance strategy for the wave glider based on the improved artificial potential field and collision prediction model. Ocean Engineering 2020, 206, 107356. https://doi.org/10.1016/j.oceaneng.2020.107356

21. Sasano M et al. Development of a semi-submersible autonomous surface vehicle for control of multiple autonomous underwater vehicles. 2016 Techno-Ocean, Kobe, Japan, 2016, pp. 309-312. https://doi.org/10.1109/techno-ocean.2016.7890667

22. Xie X et al. Development, optimization, and evaluation of a hybrid passive buoyancy compensation system for underwater gliders. Ocean Engineering 2021, 242, 110115. https://doi.org/10.1016/j.oceaneng.2021.110115

23. Fossen TI. Handbook of marine craft hydrodynamics and motion control. John Wiley & Sons; 2011. https://doi.org/10.1002/9781119994138

24. Mouring SE et al. Design of a recovery system for the SV3 wave glider. OCEANS 2017, Anchorage, AK, USA, 2017, pp. 1-6. https://doi.org/10.23919/oceans.2017.8084937